

Available online at www.synsint.com

Synthesis and Sintering

ISSN 2564-0186 (Print), ISSN 2564-0194 (Online)



Research article

Beneficial effect of low BN additive on densification and mechanical properties of hot-pressed ZrB₂–SiC composites



Saber Haghgooye Shafagh ^{a,*}, Shapour Jafargholinejad ^{id} ^b, Siyamak Javadian ^c

^a Department of Mechanical Engineering, Concordia University, Montreal, QC, H3G 1M8, Canada

^b Department of Mechanical Engineering, York University, Toronto, ON, Canada

^c Saskpower Queen Elizabeth Power Station, 2211 Spadina Cres. W., Saskatoon, SK, S7M 5V5, Canada

ABSTRACT

The incorporation of 1 wt% hexagonal BN (hBN) into ZrB₂–30 vol% SiC could noticeably better the fracture toughness, hardness, and consolidation behavior of this composite. This research intended to scrutinize the effects of various amounts of hBN (0–5 wt%) on different characteristics of ZrB₂–SiC materials. The hot-pressing method under 10 MPa at 1900 °C for 120 min was employed to sinter all designed specimens. Afterward, the as-sintered samples were characterized using X-ray diffractometry (XRD), field emission scanning electron microscopy (FESEM), energy-dispersive X-ray spectroscopy (EDS), and Vickers technique. The hBN addition up to 1 wt% improved relative density, leading to a near fully dense sample; however, the incorporation of 5 wt% of such an additive led to a composite containing more than 5% remaining porosity. The highest Vickers hardness of 23.8 GPa and fracture toughness of 5.7 MPa.m^{1/2} were secured for the sample introduced by only 1 wt% hBN. Ultimately, breaking large SiC grains, crack bridging, crack deflection, crack branching, and crack arresting were introduced as the chief toughening mechanisms in the ZrB₂–SiC–hBN system.

© 2021 The Authors. Published by Synsint Research Group.

KEYWORDS

Ultrahigh temperature ceramics
Hot-pressing
Microstructure
Mechanical properties



1. Introduction

Superior melting point, excellent hardness, high elastic modulus, and high thermal and chemical stability are some of the outstanding characteristics of zirconium diboride (ZrB₂), which have made this ultra-high-temperature ceramic (UHTC) suitable for many applications, e.g., turbine blades, cutting tools, crucibles, armor, leading edges, thermal shields, and so forth [1–4]. Besides, ZrB₂-based materials are widely used in electrical discharge devices and electrodes, owing to their acceptable thermal conductivity [5–8]. Nevertheless, poor sinterability and fracture toughness of ZrB₂ has restricted its applications to some extent, which should be addressed in one way or another [9–11].

One possible solution to tackle the poor sinterability of ZrB₂ is

implementing a modern sintering process like hot-press sintering (HP) and spark plasma sintering (SPS) in place of the conventional powder metallurgy technique [12–16]. The intrinsic characteristics of the HP and SPS routes have made them suitable to produce dense ZrB₂-based ceramics at roughly low sintering temperatures [17–20]. Furthermore, since the dwelling time of the SPS process is relatively short, the grains have not enough time to excessively grow, which may result in ceramics with improved mechanical properties [21–24]. On the other side, many scientists have tried to improve the densification behavior and mechanical features of ZrB₂ by incorporating some appropriate sintering additives. SiC, TiC, Si₃N₄, hBN, AlN, ZrO₂, sialon, and various carbonaceous phases are amongst the frequent additives studied by various researchers [25–28]. Sometimes, a chemical reaction between a secondary phase and the matrix results in forming some

* Corresponding author. E-mail address: saber.haghgooyeshafagh@concordia.ca (S. Haghgooye Shafagh)

Received 20 April 2021; Received in revised form 6 May 2021; Accepted 8 May 2021.

Peer review under responsibility of Synsint Research Group. This is an open access article under the CC BY license (<https://creativecommons.org/licenses/by/4.0/>).
<https://doi.org/10.53063/synsint.2021.1224>

nano-sized in-situ phases, which can affect the mechanical characteristics positively [29–34].

The densification behavior and microstructure of ZrB₂-SiC materials under various hot-pressing temperatures were assessed by Nguyen et al. [35]. Though the composite HPed at 1650 °C contained almost 8% remaining porosity, one sintered at 2050 °C reached its near full density, indicating the magnificent role of sintering temperature in improving the sinterability of the ZrB₂-SiC system. However, higher sintering temperature led to a rise in the average grain size of the ZrB₂ matrix and roughly doubled it. Both microstructural images and XRD spectra endorsed the unreactivity of the ZrB₂-SiC system at all three hot-pressing temperatures. On the other hand, it was found out that different mechanisms were responsible for densifying the samples sintered at various temperatures. In short, particle fragmentation and rearrangement mechanisms were governing at low hot-pressing temperatures, while the role of plastic deformation and diffusion was predominant at higher temperatures. Xia et al. [36] studied the AlN added ZrB₂-SiC materials fabricated by both pressureless sintering and hot-pressing techniques. All specimens were sintered at a similar sintering temperature of 1900 °C. Regarding the HPed samples, though the introduction of 1 wt% AlN led to a near fully dense composite, incorporating more AlN content had no noticeable effect on the relative density of ZrB₂-SiC. By contrast, more AlN weight percentage resulted in more residual porosity in the ceramics sintered by pressureless sintering method so that the 5 wt% AlN added ZrB₂-SiC sample contained almost 30% residual porosity. Besides, Nguyen et al. [37] performed a similar investigation on the ZrB₂-SiC-AlN materials under the hot-pressing conditions of 10 MPa, 120 min, and 1900 °C. Microstructural observations revealed the activation of another densification mechanism, namely liquid phase sintering, in such a system, thanks to the presence of oxide impurities on the employed starting powders. Nguyen et al. [38] also scrutinized the influence of SiC incorporation on the mechanical properties, microstructure, and consolidation of ZrB₂-hBN composites. The specimens were SPSed at 2000 °C under 30 MPa for 5 min. It was manifested that SiC has a great effect on the densification behavior of ZrB₂-hBN system, boosting relative density by more than 4%. According to their results, both sintering systems were unreactive, and only compounds associated with the original phases were present in the final ceramics. Moreover, the ternary composite was examined by the nano-indentation method, which results were as follows: hardness of ~20 GPa and elastic modulus of ~375 GPa. Finally, Wu et al. [39] assessed the impact of hBN content on various characteristics of the hBN added ZrB₂-SiC samples. They used B₄C, Si₃N₄, and ZrH₂ as the starting materials, synthesizing using the reactive SPS method at 1900 °C. Both SEM and TEM images revealed the formation of nano-sized intragranular and micro-sized intergranular hBN particles. The effect of hBN content on hardness, elastic modulus, and flexural strength of samples was highly negative. For instance, while the hardness of ceramic containing no hBN content was almost 19 GPa, it reached down to ~2 GPa for the sample with 30 vol% hBN. However, the flexural strength hit a peak at ~750 MPa when 5 vol% hBN was available in the system.

Similar to the latter research project, in this paper, we have tried to study the effect of hBN on the consolidation behavior, microstructure, fracture toughness, and hardness of ZrB₂-30 vol% SiC materials, but in low contents (0, 1, 3, and 5 wt%). Also, the ZrB₂, SiC, and hBN ingredients were utilized as the starting powders, which were hot-pressed under 10 MPa at 1900 °C for 120 min. Subsequently, the X-ray

Table 1. The list of starting materials.

| Starting powders | Particle size | Purity (%) |
|------------------|---------------|------------|
| ZrB ₂ | < 2 μm | 99.0 |
| SiC | < 5 μm | 98.0 |
| hBN | < 2 μm | 99.0 |

diffraction (XRD), field emission scanning electron microscopy (FESEM), energy-dispersive X-ray spectroscopy (EDS), and Vickers techniques were employed to characterize the HPed samples.

2. Experimental procedure

2.1. Starting materials and fabrication method

The commercially available hBN, SiC, and ZrB₂ powders were employed in this examination as the starting powders. The characteristics of these as-purchased substances are summarized in Table 1. Moreover, 4 wt% phenolic resin was added to each sample as a binder. Since the objective of this work was to evaluate the influences of hBN content on the densification behavior, microstructure, and mechanical properties of the ZrB₂-30 vol% SiC composites, four different compositions were designed to be sintered (Table 2). Initially, the ingredients of each composition were precisely weighed, and subsequently, they were dispersed mechanically in an ethanol medium by a jar-mill device. The ethanol medium was removed using a rotary evaporation facility at 90 °C. Next, the dried mixtures were ground (using an agate mortar) and screened (using a 100-mesh sieve) to attain homogenous admixtures samples. Finally, they were sintered under 10 MPa at 1900 °C for 120 min by a hot-pressing apparatus. The graphite die used in this process was lined by a double layer of graphite foil to prevent from reactions between the admixtures and the mold.

2.2. Characterization

First of all, the relative density of each sample was calculated as a proportion of its bulk and theoretical densities. Afterward, an XRD (PW1800, Philips) was employed to study the HPed specimens in terms of crystalline phases. The microstructural features of as-sintered ceramics were examined using a FESEM (Mira3, Tescan), which was armed with an EDS. The thermodynamic study was accomplished by the HSC chemical package to evaluate the feasibility of possible reactions during the sintering. Vickers technique was employed to determine fracture toughness and hardness of HPed samples by exerting 49 N loads on the polished surfaces for 14 s. For each specimen, at least six indentations were carried out. To calculate the fracture toughness values, Eq. 1 was used based on metering the length of cracks formed after indentations.

Table 2. The samples compositions.

| Sample | SiC (vol%) | hBN (wt%) |
|--------|------------|-----------|
| ZSB0 | 30 | 0 |
| ZSB1 | 30 | 1 |
| ZSB3 | 30 | 3 |
| ZSB5 | 30 | 5 |

$$K_{IC} = 0.016 \left(\frac{E}{H} \right)^{\frac{1}{2}} \left(\frac{F}{C^2} \right) \quad (1)$$

where E, H, F, and C were elastic moduli, Vickers hardness, applied force, and half of the crack length, respectively.

3. Results and discussion

One peak related to the cubic SiO₂ was identified in the XRD pattern of starting SiC powders, not shown here, endorsing the presence of surface oxide on its particles. Although no impurity phase could be detected in the XRD pattern of ZrB₂ powders, it does not mean the absence of such surface oxides. According to the literature, the surface of ZrB₂ particles is naturally covered by the ZrO₂ and B₂O₃ ingredients, which can be detrimental to the sintering behavior of ZrB₂ [40, 41]. Such impurities not only prevent from forming powerful bonding amongst the adjacent particles, but they may result in grain growth during sintering [42–44]. So, if such surface oxides can be eradicated by introducing a suitable sintering aid, both sinterability and mechanical properties of the as-sintered samples will be improved noticeably [45, 46]. The possible role of each introduced ingredient on oxide removal during hot-pressing will be discussed in the relevant section.

Fig. 1 plots relative density of the HPed specimens versus their hBN weight percentages. As is clear, the composite containing no hBN achieved a relative density of just below 97%; nevertheless, introducing 1 wt% hBN increased this number up to 99.9%, obtaining a near fully dense ceramic. By contrast, when more amount of such additive was added to the system, the relative density was diminished considerably. The lowest relative density was calculated for the sample incorporated by 5 wt% hBN, standing at 94.5%. There are several ways through which the relative density of SiC added ZrB₂ composites may be affected via the addition of hBN, including surface oxide removal, grain refining, chemical reactions, facilitating particle rearrangement, extending the range of particle size, generating gaseous phases, and so forth. In the following, such possibilities will be put into discussion.

The XRD pattern of the specimen containing 5 wt% hBN is exhibited in Fig. 2. Looking at this spectrum, just peaks of the main constituents, namely SiC, ZrB₂, and hBN, were detectable, which were in the best

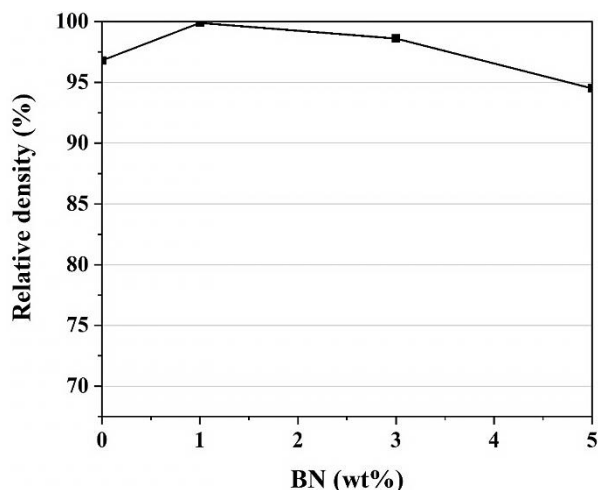


Fig. 1. The relative density changes by hBN content.

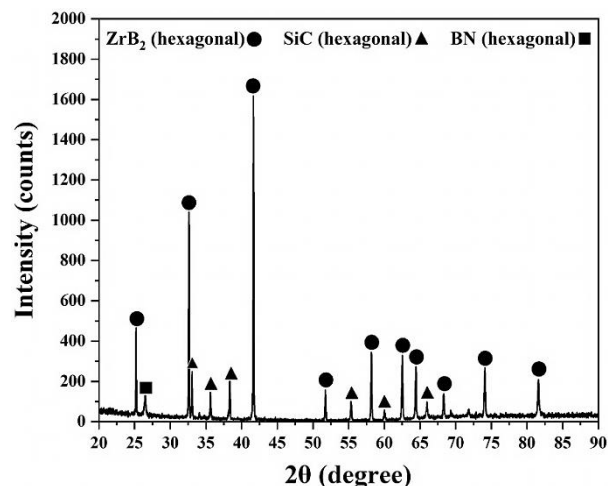
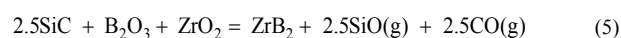
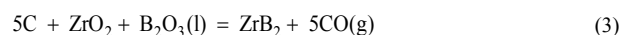


Fig. 2. The XRD spectrum of the HPed sample containing 5 wt% hBN.

agreement with the 00–034–0423, 00–029–1128, and 01–074–1978 JCPDS standards cards, respectively. As a point, it can be seen that all these compounds could preserve their initial crystalline structures, indicating their stability over the sintering working temperature. Although 4 wt% phenolic resin (equivalent to 1.6 wt% pyrolyzed carbon) had been added to the system as a binder, no peak associated with graphite could be identified in the attributing XRD pattern. It may imply the full consumption of such a phase over the hot-pressing. This phenomenon could happen over the eradication of surface impurities. As noted earlier, ZrO₂, B₂O₃, and SiO₂ are the main surface oxides in the ZrB₂–SiC–hBN system. B₂O₃ is an ingredient with a low melting point, which is in the liquid state at temperatures higher than almost 450 °C (Eq. 2). This liquid oxide, together with ZrO₂, may participate in a reaction with pyrolyzed carbon according to Eq. 3. The products of such equivalence are in-situ ZrB₂, and the gaseous phase of CO, which can escape from the system owing to the applied vacuum. Fig. 3 endorses the feasibility of this reaction at temperatures higher than around 1500 °C. Also, all the oxide ingredients may be reduced in a single reaction by the pyrolyzed carbon based on Eq. 4, converting to the in-situ ZrB₂ and SiC compounds. Similar to the previous reaction, Eq. 3 can also proceed at sintering temperatures over ~1500 °C (Fig. 3). On the other hand, the oxide removal phenomenon may take place in the absence of carbon as a reductant agent. Based on Eq. 5, the SiC reinforcement can play the role of graphite in reducing ZrO₂ and B₂O₃ ingredients. The products in this equation are in-situ ZrB₂, together with two gaseous phases of SiO and CO. Fig. 3 endorses the favorability of this reaction under the current hot-pressing circumstances. The advancement of Eqs. 2–5 can improve the densification behavior of the ZrB₂–SiC–hBN system in two different ways. One is associated with the role of the produced in-situ phases in removing residual pores. Another is preventing excessive grain growth, thanks to the surface oxide removal.



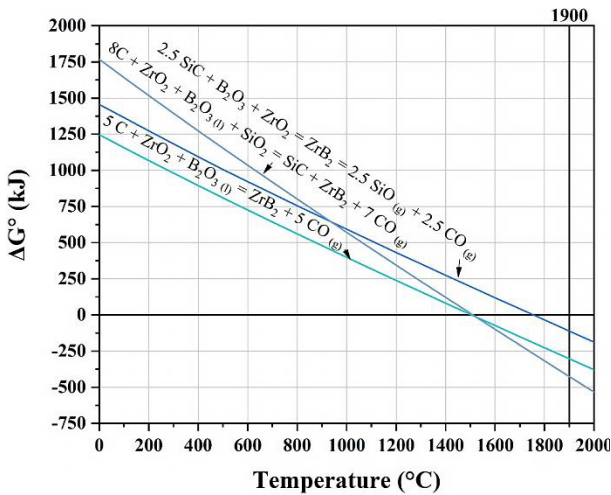


Fig. 3. The temperature dependency of ΔG° for Eqs. 3–5.

However, why hBN in low and high contents had different impacts on the densification behavior of ZrB_2 –SiC should be clarified. The hBN particles possessed a range of sizes in contrary to ZrB_2 and SiC, which were roughly uniform. So, this characteristic could be helpful in filling the free spaces amongst the larger particles. On the other hand, hBN is a relatively soft phase, which is even used for lubrication purposes [47]. Accordingly, the presence of it in a system may facilitate particle rearrangement as a densification mechanism. Moreover, as a stable species in the present sintering system, it could significantly promote grain refining as another consolidation mechanism. Nevertheless, hBN has some deficiencies, too, which can be detrimental in higher amounts. Although the starting hBN is comprised of fine particles, the new hBN platelets were possibly formed through nucleation and

growth mechanisms. Since the hBN platelets grow two-dimensionally and only a weak Van der Waals force bond them together, the possibility of gas entrapment between their sheets exists. This would be worse when a few bunches of hBN sheets grow in the vicinity of each other, generating a considerable amount of residual porosity. This issue can be the main reason for the lower relative density of samples with higher contents of hBN in comparison with that introduced by only 1 wt% hBN.

Figs. 4a–c illustrates the polished surfaces FESEM images of samples incorporated by 1–5 wt% hBN. Considering the EDS map results presented in Fig. 5, it is obvious that the microstructures of all these three composites are mainly consisted of the SiC reinforcement (dark-colored phase) and the ZrB_2 matrix (bright-colored phase). Due to the two-dimensional growth of new hBN platelets, detecting them on the polished surfaces of specimens is somehow difficult. However, they can be easily observed in the samples fractographs in Figs. 4d–f. Looking at Fig. 4d, the beneficial role of low content hBN is apparent. The HPed sample is quite dense and any porosity can be seen in neither grain boundaries nor triple pockets. In this ceramic, some single bunches of hBN platelets can be observed that are mainly surrounded by the ZrB_2 matrix or the SiC reinforcement. Thanks to the low content of hBN, this additive could be dispersed all over the microstructure, contributing to filling the residual porosity. However, the issue was different in higher weight percentages of hBN, as can be ascertained in Figs. 4e, f. The growth of various bunches of hBN sheets with different orientations in some specific zones led to gas entrapment in such places, and consequently the promotion of remaining porosity. This microstructural observation is in a great harmony with the values achieved for the relative density. Regarding fracture modes, both inter- and intragranular fracture types can be observed in the fracture surfaces of all three composites (Figs. 4e, f). Such mixed fracture mode can be beneficial in strengthening such composite specimens.

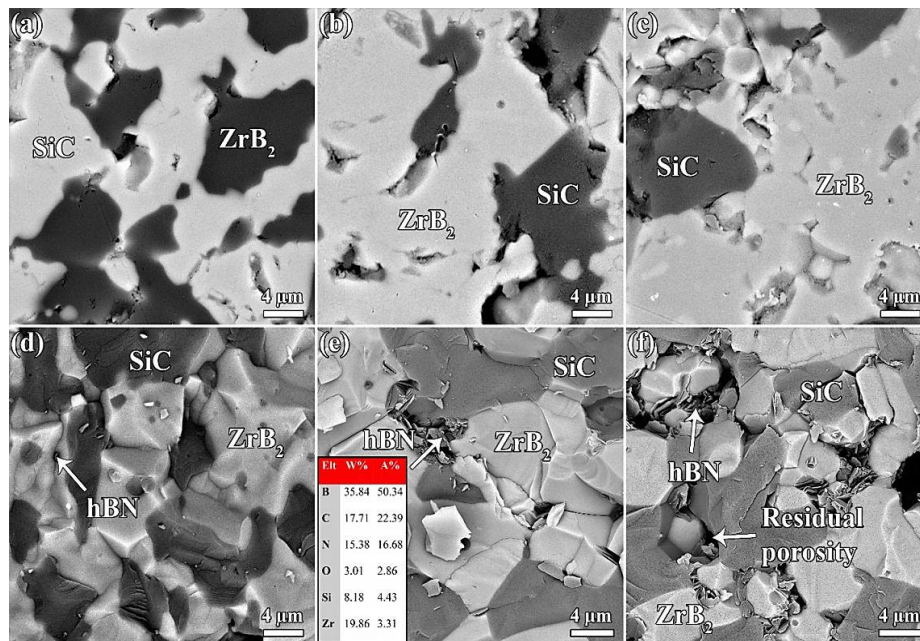


Fig. 4. The backscattered FESEM micrographs from both polished and fracture surfaces of the a, d) ZSB1, b, e) ZSB3, and c, f) ZSB5 ceramics.

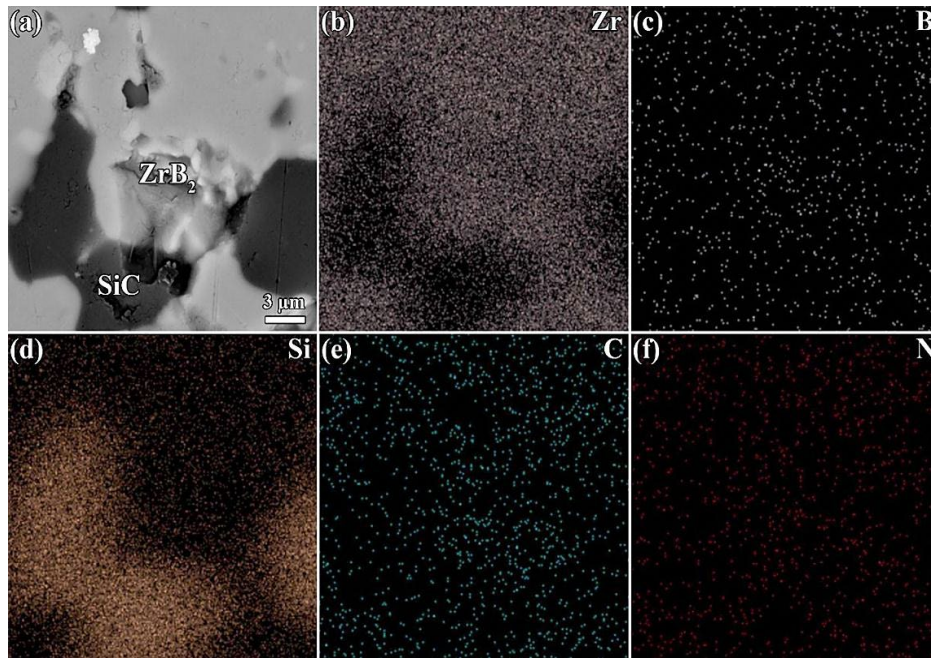


Fig. 5. The polished surfaces FESEM micrograph of the ZSB1 ceramic, together with the corresponding EDS maps.

Fig. 6 indicates the hBN content dependency of mechanical properties of the HPed samples. The hBN-free composite secured a Vickers hardness of 19.2 GPa; however, the incorporation of 1 wt% hBN could improve the hardness of the ZrB₂-SiC system by almost 23%, standing at 23.8 GPa. Similar to the relative density trend, introducing more hBN additive resulted in lower Vickers hardness values. The lowest hardness of almost 18 GPa was related to the composite with the highest hBN content, namely 5 wt%. Considering all the possible causes, it seems that the residual porosity was the most predominant factor in determining the hardness values of specimens. It is true that hBN is a soft phase; nevertheless, it could improve the relative density by ~3% in the ZSB1 ceramic. Furthermore, such an additive could possibly contribute to grain refining, which can significantly affect the hardness of a ceramic-based material. Regarding the samples containing more hBN content, apart from the controlling role of

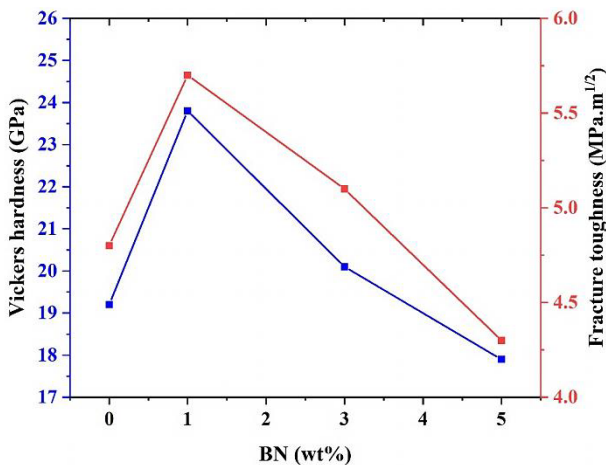


Fig. 6. The Vickers hardness and fracture toughness of HPed ceramics.

relative density, the impact of the existence of a soft phase (hBN) in the microstructure should not be overlooked.

Fig. 6 also plots the fracture toughness values of the HPed materials based on their hBN contents. As can be seen, the trend of this characteristic is in harmony with those for relative density and Vickers hardness. According to this graph, the lowest (4.3 MPa.m^{1/2}) and highest (5.7 MPa.m^{1/2}) values of fracture toughness were related to the

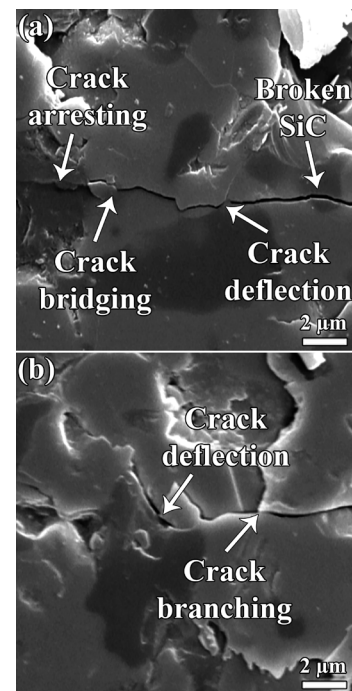


Fig. 7. The indentation crack paths on the polished surface of the ZSB5 composite.

samples with 5 and 1 wt% hBN, respectively. Although the addition of more content of a secondary phase like hBN may improve fracture toughness via different mechanisms, such as crack branching, crack arresting, crack bridging, crack deflection, etc., it seems that the residual porosity was the controlling factor in this feature, too. The various toughening mechanisms activated in the ZSB5 sample is illustrated in Fig. 7. Apart from the mentioned mechanisms above, it is clear that breaking large SiC grains was also played as a toughening mechanism, too.

4. Conclusions

The impacts of different amounts of hBN (0, 1, 3, and 5 wt%) on the mechanical properties, densification behavior, and microstructural development of ZrB₂-30 vol% SiC material were studied in this investigation. All samples were sintered at the same sintering conditions of 10 MPa, 1900 °C, and 120 min using the hot-pressing technique. Although the incorporation of 1 wt% hBN promoted the relative density, attaining a near fully dense composite, the addition of more hBN amounts diminished the relative density considerably. The role of hBN in grain refining, facilitating particle rearrangement, and extending the range of particle sizes of prepared admixture was suggested as the possible causes that resulted in enhancing the consolidation behavior at low hBN content. However, when more hBN weight percentages were added to the system, various bunches of hBN platelets with different orientations grew in the vicinity of each other, leading to gas entrapment in such areas, and as a result, a decrease in the relative density value. The best Vickers hardness of 23.8 GPa and fracture toughness of 5.7 MPa.m^{1/2} were achieved for the specimen containing 1 wt% hBN. Finally, crack deflection, crack arresting, crack bridging, crack branching, and breaking large SiC grains were introduced as the main toughening mechanisms in the ZrB₂-SiC-hBN composites.

CRedit authorship contribution statement

Saber Haghgooye Shafagh: Conceptualization, Investigation, Writing – original draft.

Shapour Jafarholnejad: Supervision, Methodology, Resources.

Siyamak Javadian: Validation, Writing – review & editing.

Data availability

The data underlying this article will be shared on reasonable request to the corresponding author.

Declaration of competing interest

The authors declare no competing interests.

Funding and acknowledgment

The authors would like to thank Concordia University and York University for supporting this research.

References

- [1] O. Popov, J. Vleugels, E. Zeynalov, V. Vishnyakov, Reactive hot pressing route for dense ZrB₂-SiC and ZrB₂-SiC-CNT ultra-high temperature ceramics, *J. Eur. Ceram. Soc.* 40 (2020) 5012–5019. <https://doi.org/10.1016/j.jeurceramsoc.2020.07.039>.
- [2] Z. Balak, M. Zakeri, M.R. Rahimpur, E. Salahi, H. Nasiri, Effect of open porosity on flexural strength and hardness of ZrB₂-based composites, *Ceram. Int.* 41 (2015) 8312–8319. <https://doi.org/10.1016/j.ceramint.2015.02.143>.
- [3] R. Eatemadi, Z. Balak, Investigating the effect of SPS parameters on densification and fracture toughness of ZrB₂-SiC nanocomposite, *Ceram. Int.* 45 (2019) 4763–4770. <https://doi.org/10.1016/j.ceramint.2018.11.169>.
- [4] X. Ren, H. Chu, K. Wu, A. Zhang, M. Huang, et al., Effect of the ZrB₂ content on the oxygen blocking ability of ZrB₂-SiC coating at 1973K, *J. Eur. Ceram. Soc.* 41 (2021) 1059–1070. <https://doi.org/10.1016/j.jeurceramsoc.2020.10.036>.
- [5] M. Shahedi Asl, A. Sabahi Namini, S.A. Delbari, Q.V. Le, M. Shokouhimehr, M. Mohammadi, A TEM study on the microstructure of spark plasma sintered ZrB₂-based composite with nano-sized SiC dopant, *Prog. Nat. Sci. Mater. Int.* 31 (2021) 47–54. <https://doi.org/10.1016/j.pnsc.2020.11.010>.
- [6] X. Pan, C. Li, Y. Niu, X. Zhong, L. Huang, et al., Effect of Yb₂O₃ addition on oxidation/ablation behaviors of ZrB₂-MoSi₂ composite coating under different environment, *Corros. Sci.* 175 (2020) 108882. <https://doi.org/10.1016/j.corsci.2020.108882>.
- [7] R. Hassan, R. Kundu, K. Balani, Oxidation behaviour of coarse and fine SiC reinforced ZrB₂ at re-entry and atmospheric oxygen pressures, *Ceram. Int.* 46 (2020) 11056–11065. <https://doi.org/10.1016/j.ceramint.2020.01.125>.
- [8] A.D. Stanfield, G.E. Hilmas, W.G. Fahrenholtz, Effects of Ti, Y, and Hf additions on the thermal properties of ZrB₂, *J. Eur. Ceram. Soc.* 40 (2020) 3824–3828. <https://doi.org/10.1016/j.jeurceramsoc.2020.04.011>.
- [9] T.P. Nguyen, M. Ghassemi Kakroudi, M. Shahedi Asl, Z. Ahmadi, A. Sabahi Namini, et al., Influence of SiAlON addition on the microstructure development of hot-pressed ZrB₂-SiC composites, *Ceram. Int.* 46 (2020) 19209–19216. <https://doi.org/10.1016/j.ceramint.2020.04.258>.
- [10] A. Vinci, L. Zoli, P. Galizia, D. Sciti, Influence of Y₂O₃ addition on the mechanical and oxidation behaviour of carbon fibre reinforced ZrB₂/SiC composites, *J. Eur. Ceram. Soc.* 40 (2020) 5067–5075. <https://doi.org/10.1016/j.jeurceramsoc.2020.06.043>.
- [11] H.J. Ding, X.G. Wang, J.F. Xia, W.C. Bao, G.J. Zhang, et al., Effect of solid solution and boron vacancy on the microstructural evolution and high temperature strength of W-doped ZrB₂ ceramics, *J. Alloys Compd.* 827 (2020) 154293. <https://doi.org/10.1016/j.jallcom.2020.154293>.
- [12] H. Aghajani, E. Hadavand, N.S. Peighambaridou, S. Khameneh asl, Electro spark deposition of WC-TiC-Co-Ni cermet coatings on St52 steel, *Surf. Interfaces* 18 (2020) 100392. <https://doi.org/10.1016/j.surf.2019.100392>.
- [13] Z. Balak, M. Azizieh, H. Kafashan, M. Shahedi Asl, Z. Ahmadi, Optimization of effective parameters on thermal shock resistance of ZrB₂-SiC-based composites prepared by SPS: using Taguchi design, *Mater. Chem. Phys.* 196 (2017) 333–340. <https://doi.org/10.1016/j.matchemphys.2017.04.062>.
- [14] Z. Balak, Shrinkage, hardness and fracture toughness of ternary ZrB₂-SiC-HfB₂ composite with different amount of HfB₂, *Mater. Chem. Phys.* 235 (2019) 121706. <https://doi.org/10.1016/j.matchemphys.2019.05.094>.
- [15] S.K. Kashyap, R. Mitra, Densification behavior involving creep during spark plasma sintering of ZrB₂-SiC based ultra-high temperature ceramic composites, *Ceram. Int.* 46 (2020) 5028–5036. <https://doi.org/10.1016/j.ceramint.2019.10.246>.
- [16] S.A. Akbarpour Shalmani, M. Sobhani, O. Mirzaee, M. Zakeri, Effect of HfB₂ and WC additives on the ablation resistance of ZrB₂-SiC composite coating manufactured by SPS, *Ceram. Int.* 46 (2020) 25106–25112. <https://doi.org/10.1016/j.ceramint.2020.06.297>.
- [17] X. Zhao, Z. Chen, H. Wang, Z. Zhang, G. Shao, et al., The influence of additive and temperature on thermal shock resistance of ZrB₂ based composites fabricated by Spark Plasma Sintering, *Mater.*

- Chem. Phys. 240 (2020) 122061.
<https://doi.org/10.1016/j.matchemphys.2019.122061>.
- [18] T.P. Nguyen, M. Shahedi Asl, S.A. Delbari, A. Sabahi Namini, Q.V. Le, et al., Electron microscopy investigation of spark plasma sintered ZrO₂ added ZrB₂-SiC composite, *Ceram. Int.* 46 (2020) 19646–19649. <https://doi.org/10.1016/j.ceramint.2020.04.292>.
- [19] Z. Balak, M. Zakeri, Effect of HfB₂ on microstructure and mechanical properties of ZrB₂-SiC-based composites, *Int. J. Refract. Met. Hard Mater.* 54 (2016) 127–137. <https://doi.org/10.1016/j.jirmhm.2015.07.011>.
- [20] P. Sengupta, S.S. Sahoo, A. Bhattacharjee, S. Basu, I. Manna, Effect of TiC addition on structure and properties of spark plasma sintered ZrB₂-SiC-TiC ultrahigh temperature ceramic composite, *J. Alloys Compd.* 850 (2021) 156668. <https://doi.org/10.1016/j.jallcom.2020.156668>.
- [21] V.H. Nguyen, A. Sabahi Namini, S.A. Delbari, Q.V. Le, M. Shahedi Asl, et al., A survey on spark plasma sinterability of CNT-added TiC ceramics, *Int. J. Refract. Met. Hard Mater.* (2021) 105471. <https://doi.org/10.1016/j.jirmhm.2021.105471>.
- [22] N. Sadeghi, M.R. Akbarpour, H. Aghajani, A novel two-step mechanical milling approach and in-situ reactive synthesis to fabricate TiC/Graphene layer/Cu nanocomposites and investigation of their mechanical properties, *Mater. Sci. Eng. A.* 734 (2018) 164–170. <https://doi.org/10.1016/j.msea.2018.07.101>.
- [23] Z. Balak, M. Zakeri, Application of Taguchi L32 orthogonal design to optimize flexural strength of ZrB₂-based composites prepared by spark plasma sintering, *Int. J. Refract. Met. Hard Mater.* 55 (2016) 58–67. <https://doi.org/10.1016/j.jirmhm.2015.11.009>.
- [24] P. Vaziri, Z. Balak, Improved mechanical properties of ZrB₂-30 vol% SiC using zirconium carbide additive, *Int. J. Refract. Met. Hard Mater.* 83 (2019) 104958. <https://doi.org/10.1016/j.jirmhm.2019.05.004>.
- [25] C. Xia, M. Shahedi Asl, A. Sabahi Namini, Z. Ahmadi, S.A. Delbari, et al., Enhanced fracture toughness of ZrB₂-SiCw ceramics with graphene nano-platelets, *Ceram. Int.* 46 (2020) 24906–24915. <https://doi.org/10.1016/j.ceramint.2020.06.275>.
- [26] S. Sun, Y. Liu, Z. Ma, S. Zhu, C. Hong, et al., Fabrication of ZrB₂-SiC powder with a eutectic phase for sintering or plasma spraying, *Powder Technol.* 372 (2020) 506–518. <https://doi.org/10.1016/j.powtec.2020.06.019>.
- [27] T.D. Le, K. Hirota, M. Kato, H. Miyamoto, M. Yuasa, T. Nishimura, Fabrication of dense ZrB₂/B₄C composites using pulsed electric current pressure sintering and evaluation of their high-temperature bending strength, *Ceram. Int.* 46 (2020) 18478–18486. <https://doi.org/10.1016/j.ceramint.2020.04.153>.
- [28] J. Zou, G.J. Zhang, Z.Y. Fu, In-situ ZrB₂-hBN ceramics with high strength and low elasticity, *J. Mater. Sci. Technol.* 48 (2020) 186–193. <https://doi.org/10.1016/j.jmst.2020.01.061>.
- [29] A. Razmjou, M. Asadnia, E. Hosseini, A. Habibnejad Korayem, V. Chen, Design principles of ion selective nanostructured membranes for the extraction of lithium ions, *Nat. Commun.* 10 (2019) 5793. <https://doi.org/10.1038/s41467-019-13648-7>.
- [30] H. Karimi-Maleh, B.G. Kumar, S. Rajendran, J. Qin, S. Vadivel, et al., Tuning of metal oxides photocatalytic performance using Ag nanoparticles integration, *J. Mol. Liq.* 314 (2020) 113588. <https://doi.org/10.1016/j.molliq.2020.113588>.
- [31] H. Karimi Maleh, F. Karimi, M. Alizadeh, A.L. Sanati, Electrochemical Sensors, a Bright Future in the Fabrication of Portable Kits in Analytical Systems, *Chem. Rec.* 20 (2020) 682–692. <https://doi.org/10.1002/tcr.201900092>.
- [32] N. Sadeghi, H. Aghajani, M.R. Akbarpour, Microstructure and tribological properties of in-situ TiC-C/Cu nanocomposites synthesized using different carbon sources (graphite, carbon nanotube and graphene) in the Cu-Ti-C system, *Ceram. Int.* 44 (2018) 22059–22067. <https://doi.org/10.1016/j.ceramint.2018.08.316>.
- [33] F. Tahernejad Javazmi, M. Shabani-Nooshabadi, H. Karimi Maleh, 3D reduced graphene oxide/FeNi₃-ionic liquid nanocomposite modified sensor; an electrical synergic effect for development of tert-butylhydroquinone and folic acid sensor, *Compos. Part B Eng.* 172 (2019) 666–670. <https://doi.org/10.1016/j.compositesb.2019.05.065>.
- [34] A. Razmjou, M. Asadnia, O. Ghaebi, H.C. Yang, M. Ebrahimi Warkiani, et al., Preparation of Iridescent 2D Photonic Crystals by Using a Mussel-Inspired Spatial Patterning of ZIF-8 with Potential Applications in Optical Switch and Chemical Sensor, *ACS Appl. Mater. Interfaces.* 9 (2017) 38076–38080. <https://doi.org/10.1021/acsami.7b13618>.
- [35] V.H. Nguyen, S.A. Delbari, M. Shahedi Asl, A. Sabahi Namini, M. Ghassemi Kakroudi, et al., Role of hot-pressing temperature on densification and microstructure of ZrB₂-SiC ultrahigh temperature ceramics, *Int. J. Refract. Met. Hard Mater.* 93 (2020) 105355. <https://doi.org/10.1016/j.jirmhm.2020.105355>.
- [36] C. Xia, S.A. Delbari, Z. Ahmadi, M. Shahedi Asl, M. Ghassemi Kakroudi, et al., Electron microscopy study of ZrB₂-SiC-AlN composites: Hot-pressing vs. pressureless sintering, *Ceram. Int.* 46 (2020) 29334–29338. <https://doi.org/10.1016/j.ceramint.2020.08.054>.
- [37] V.H. Nguyen, S.A. Delbari, Z. Ahmadi, M. Shahedi Asl, M. Ghassemi Kakroudi, et al., TEM characterization of hot-pressed ZrB₂-SiC-AlN composites, *Results Phys.* 19 (2020) 103348. <https://doi.org/10.1016/j.rinp.2020.103348>.
- [38] V.H. Nguyen, M. Shahedi Asl, S.A. Delbari, Q.V. Le, A. Sabahi Namini, et al., Effects of SiC on densification, microstructure and nano-indentation properties of ZrB₂-BN composites, *Ceram. Int.* 47 (2020) 9873–9880. <https://doi.org/10.1016/j.ceramint.2020.12.129>.
- [39] W.W. Wu, M. Estili, T. Nishimura, G.J. Zhang, Y. Sakka, Machinable ZrB₂-SiC-BN composites fabricated by reactive spark plasma sintering, *Mater. Sci. Eng. A.* 582 (2013) 41–46. <https://doi.org/10.1016/j.msea.2013.05.079>.
- [40] S. Jafari, M. Bavand Vandchali, M. Mashhadi, A. Nemati, Effects of HfB₂ addition on pressureless sintering behavior and microstructure of ZrB₂-SiC composites, *Int. J. Refract. Met. Hard Mater.* 94 (2021) 105371. <https://doi.org/10.1016/j.jirmhm.2020.105371>.
- [41] S. Mandal, A. Pramanick, S. Chakraborty, P. Pratim Dey, Phase determination of ZrB₂-B₄C ceramic composite material using XRD and rietveld refinement analysis, *Mater. Today Proc.* 33 (2020) 5664–5666. <https://doi.org/10.1016/j.matpr.2020.04.124>.
- [42] H. Karimi Maleh, M. Sheikshoae, I. Sheikshoae, M. Ranjbar, J. Alizadeh, et al., A novel electrochemical epinine sensor using amplified CuO nanoparticles and a n-hexyl-3-methylimidazolium hexafluorophosphate electrode, *New J. Chem.* 43 (2019) 2362–2367. <https://doi.org/10.1039/C8NJ0581E>.
- [43] Z. Taherian, A. Khataee, Y. Orooji, Facile synthesis of yttria-promoted nickel catalysts supported on MgO-MCM-41 for syngas production from greenhouse gases, *Renew. Sustain. Energy Rev.* 134 (2020) 110130. <https://doi.org/10.1016/j.rser.2020.110130>.
- [44] A. Yazdani, M. Soltanieh, H. Aghajani, Structural and mechanical evaluation of deposited nano structured TiN coating using active screen plasma nitriding technique, *Eur. Phys. J. Appl. Phys.* 65 (2014) 20801. <https://doi.org/10.1051/epjap/2014130095>.
- [45] H. Karimi Maleh, K. Cellat, K. Arıkan, A. Savk, F. Karimi, F. Şen, Palladium-Nickel nanoparticles decorated on Functionalized-MWCNT for high precision non-enzymatic glucose sensing, *Mater. Chem. Phys.* 250 (2020) 123042. <https://doi.org/10.1016/j.matchemphys.2020.123042>.
- [46] M. Ahmadi, H. Aghajani, Suspension characterization and electrophoretic deposition of Yttria-stabilized Zirconia nanoparticles on an iron-nickel based superalloy, *Ceram. Int.* 43 (2017) 7321–7328. <https://doi.org/10.1016/j.ceramint.2017.03.035>.
- [47] N. Pourmohammadi Vafa, M. Ghassemi Kakroudi, M. Shahedi Asl, Role of h-BN content on microstructure and mechanical properties of hot-pressed ZrB₂-SiC composites, *Ceram. Int.* 46 (2020) 21533–21541. <https://doi.org/10.1016/j.ceramint.2020.05.255>.